Supporting Information

The NICS Values Scan in Three-dimensional Space of the hoop-shaped π-conjugated molecules:

[6]$_8$cyclacene and [16]trannulene

Qing Li,[a,b] Hong-Liang Xu[a*]   and Zhong-Min Su [a,b, *]

aInstitute of Functional Material Chemistry, Faculty of Chemistry, Northeast Normal University, Changchun,

Jilin 130024, China.

bDepartment of Chemistry, Faculty of Science, Yanbian University, Yanji, Jilin, 133002, China.

Contents

19. The situation between the internal magnetic field during the course of two [16]trannulenes stacked into [6]$_8$cyclacene.

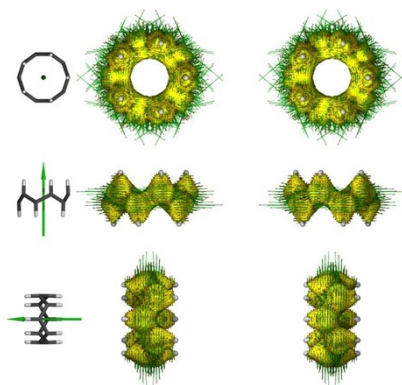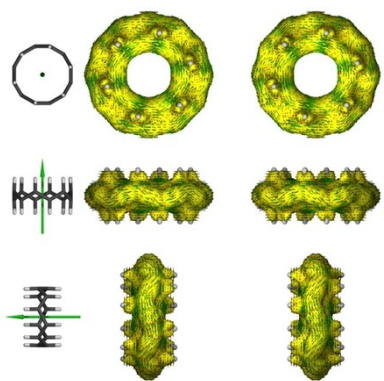**Figure S1.** The ACID of [**10**]trannulene.

Figure S2. The ACID of [**12**]trannulene.
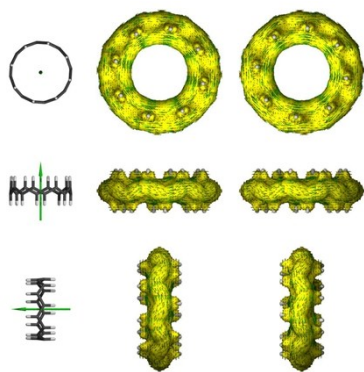
Figure S3. The ACID of [**14**]trannulene.
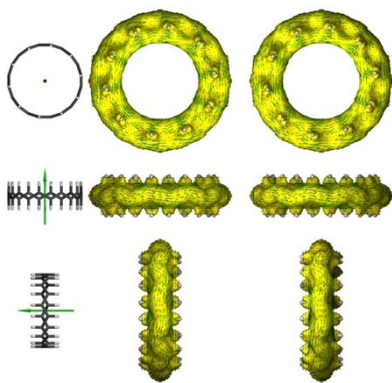
Figure S4. The ACID of [**20**]trannulene.
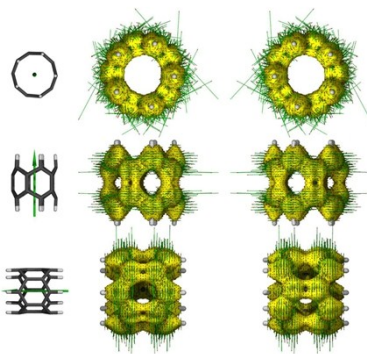
Figure S5. The ACID of [**6**]₅cyclacene.
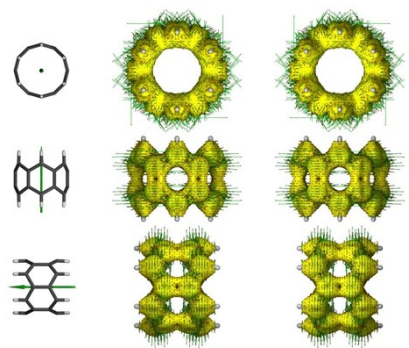
Figure S6. The ACID of [**6**]₆cyclacene.
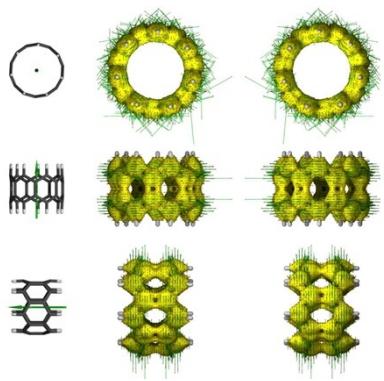
Figure S7. The ACID of [**6**]₇cyclacene.
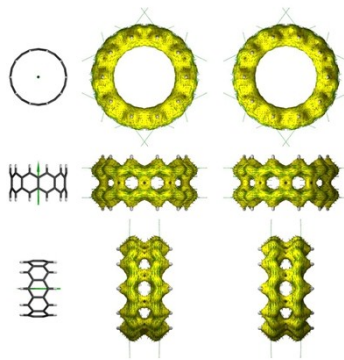
Figure S8. The ACID of [**6**]$_{10}$cyclacene.
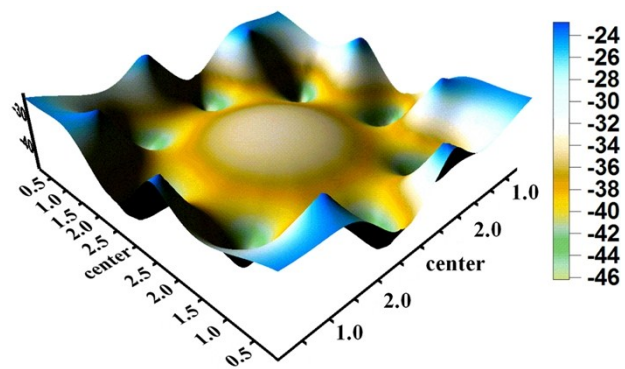
Figure S9. The planar NICS values scan of **P(L=0.2)** for [**6**]$_8$cyclacene.
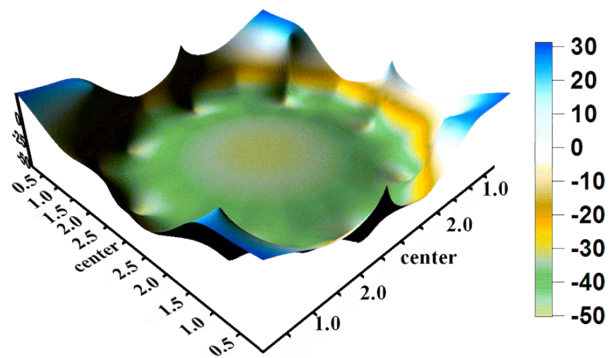
Figure S10. The planar NICS values scan of **P(L=0.6)** for [**6**]$_8$cyclacene.
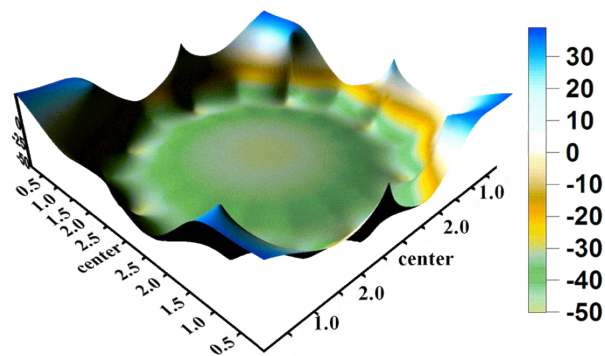
Figure S11. The planar NICS values scan of **P(L=0.8)** for [**6**]$_8$cyclacene.
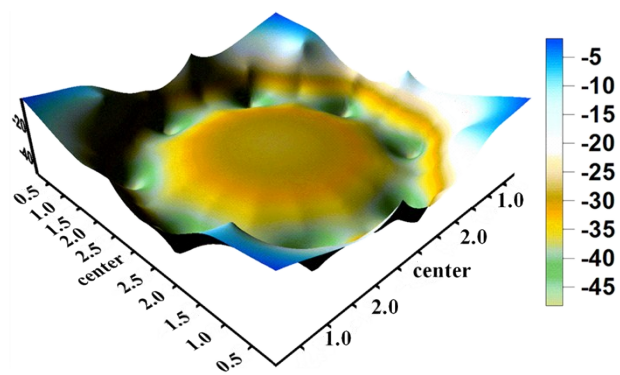
Figure S12. The planar NICS values scan of **P(L=1.2)** for [**6**]$_8$cyclacene.
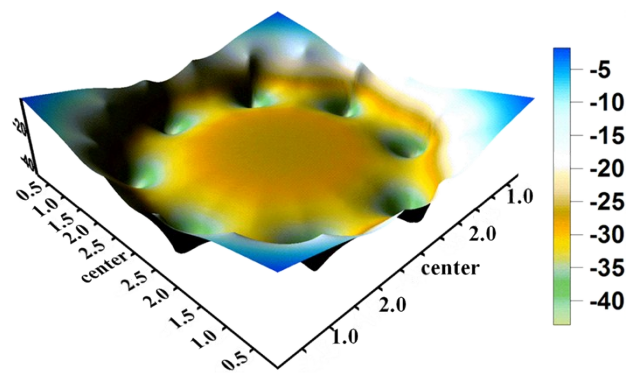
Figure S13. The planar NICS values scan of **P(L=1.4)** for [**6**]$_8$cyclacene.
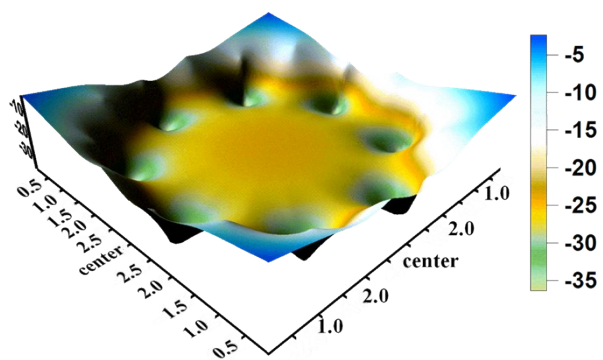
Figure S14. The planar NICS values scan of **P(L=1.6)** for [**6**]₈cyclacene.
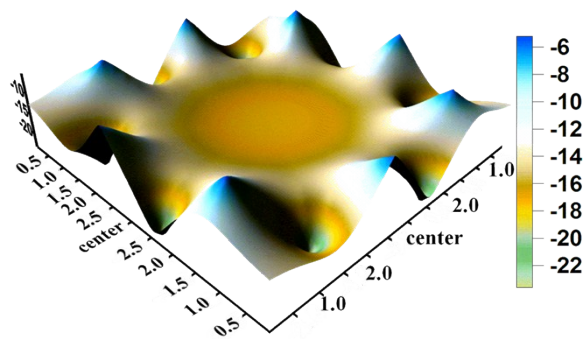
Figure S15. The planar NICS values scan of **P(L=2.4)** for [**6**]$_8$cyclacene.

Figure S16. The planar NICS values scan of **P(L=2.6)** for [**6**]$_8$cyclacene.

Figure S17. The planar NICS values scan of **P(L=2.8)** for [**6**]$_8$cyclacene.
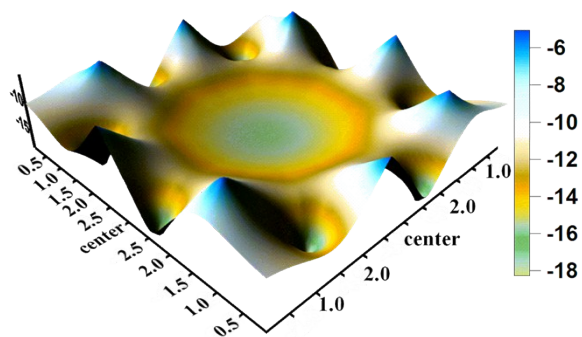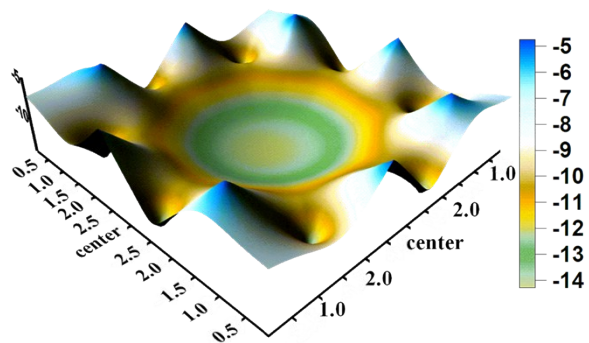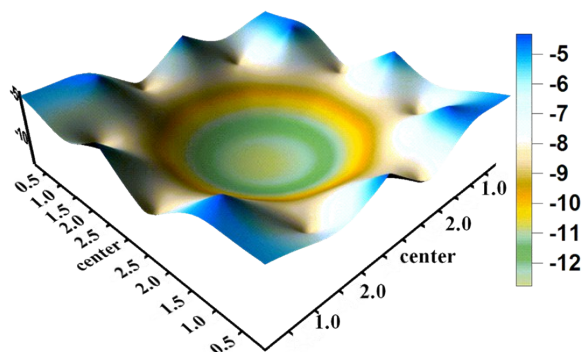
Figure S18. The planar NICS values scan of **P(L=3.0)** for [**6**]$_8$cyclacene.

The situation between the internal magnetic field during the course of two [16]trannulenes stacked into [6]$_8$cyclacene.
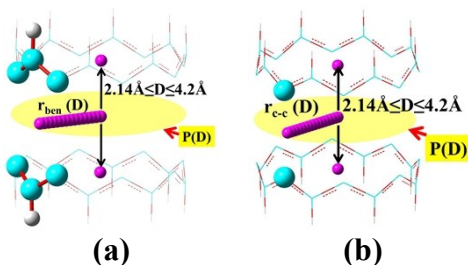

(a)   **(b)**

Figure S19. The diagram for the NICS values scan about the center cross-section **P(D**=2.14~4.20Å) in the stack process.

In order to explicitly describe the situation between the internal magnetic field during the course of two [**16**]trannulenes stacked into [**6**]$_8$cyclacene. We simulated the change of the center cross-section internal magnetic field in the stack process by the NICS values scan method. Firstly, the center cross-section is defined as **P(D**=2.14~4.20Å), in which **D** (2.14~4.20Å) is defined as the distance of two [**16**]trannulenes in the stack process (Figure S19). On the other hand, the two kinds radius (**r$_{ben}$(D**=2.14~4.20Å) and **r$_{c-c}$(D**=2.14~4.20Å)) in center cross-section are listed in Figure S19. The distance from the center of the six-member ring to the center of the cross-section is represented by the **r$_{ben}$(D**=2.14~4.20Å), and the distance from the center of the C-C bond to the center of the cross-section is represented by the **r$_{c-c}$(D**=2.14~4.20Å).

P(D=4.20)   P(D=3.70)   P(D=3.20)   P(D=2.70)   P(D=2.14)

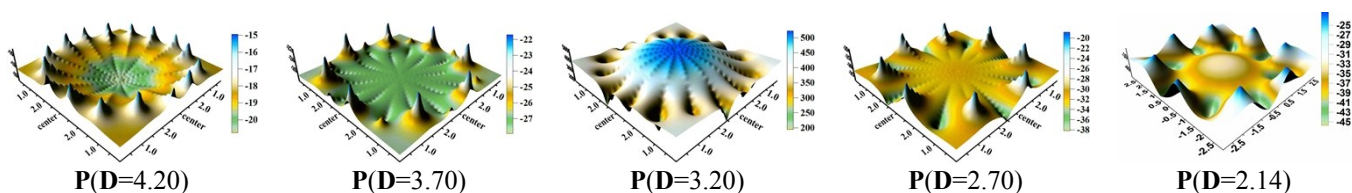**Figure S20.** The NICS scan in the cross-section **P(D**=2.14~4.20Å).

Figure S20 lists the typical schematic diagram of the NICS values scan in the center cross-section $P(D=2.14\sim4.20)$ based on the results of the NICS values scan in the $r_{ben}(D=2.14\sim4.20)$ and $r_{c-c}(D=2.14\sim4.20)$. There is a significant difference of the internal magnetic field with one [16]trannulenes closed to another [16]trannulenes. When $D>3.2$Å, there is a induced aromaticity due to the influence of two [16]trannulenes, and the aromaticity is enhancing with the D decreasing. However, when $D\approx3.2$Å, the drastic anti-aromaticity has existed between two [16]trannulenes. With the formation of [6]$_8$cyclacene, the obvious aromaticity has been appeared gradually.